Behavior of flowing granular materials under variable *g*

Antje Brucks,[1,*] Tim Arndt,[1] Julio M. Ottino,[2,3] and Richard M. Lueptow[3,†]
[1]*Zentrum für Angewandte Raumfahrttechnologie und Mikrogravitation (ZARM), Universität Bremen, Am Fallturm, 28359 Bremen, Germany*
[2]*Department of Chemical and Biological Engineering, Northwestern University, Evanston, Illinois 60208, USA*
[3]*Department of Mechanical Engineering, Northwestern University, Evanston, Illinois 60208, USA*
(Received 18 August 2006; revised manuscript received 26 January 2007; published 28 March 2007)

We consider the impact of the effective gravitational acceleration g_{eff} on gravity-driven granular shear flow utilizing a tumbler of radius R rotating at angular velocity ω when g_{eff} is varied up to 25 times the gravitational level on Earth in a large centrifuge. The Froude number $\mathrm{Fr}=\omega^2 R/g_{eff}$ is shown to be the proper scaling to characterize the effect of gravity on the angle of repose of the flowing layer. Likewise, transitions between flow regimes depend on Fr. Furthermore, the thickness of the flowing layer is independent of the g level. These results provide a starting point for understanding granular flows on planetary bodies with g_{eff} different than on Earth for application to planetary exploration and formation of geologic features.

DOI: 10.1103/PhysRevE.75.032301 PACS number(s): 45.70.−n, 47.57.Gc

Gravity is the determinant factor in most granular shear flows from geologic situations (including landslides and sandpiles on a beach) to industrial applications (processing of grains, ores, and pharmaceuticals), but the effect of changing the gravitational acceleration is largely unexplored. Gravity-driven flow of granular materials is particularly important in the understanding of the geology of planets as well as for human exploration and construction on the Moon and Mars in the next decades. For example, surface features on Mars [1–4], Venus [5,6], and other planetary bodies [7,8] are thought to be the result of avalanches of loose granular material. Likewise, the exploration of the Moon and Mars in the next two decades will require the deployment of landing and exploration vehicles on surfaces of loose granular material and may involve excavation or incorporate *in situ* resource utilization of surface material [9]. Thus, the impact of the gravitational acceleration on granular flow is of importance for understanding the geology of other planets and to clarify the environments that may be encountered during planetary exploration. The results presented here provide the proper dimensionless scaling for the effect of gravity on granular flow and provide the starting point for further investigations of the thickness, dilation, velocity, and shear in the flowing layer, as well as the nature of the creeping subsurface flow under varying levels of gravitational acceleration.

An ideal study of gravitational effects related to the geology of planets and issues of moving granular materials for construction of human habitats should include granular surface shear flows related to heaping and avalanching. However, it is difficult to experimentally consider these situations at varying gravitational levels. Granular flow in a rotating tumbler is dominated by surface shear flows, similar to flows in heaping and avalanching. Therefore, we consider the flowing shear layer for the canonical case of granular flow in a tumbler when the gravitational acceleration g is varied up to 25 times that on Earth in the large centrifuge shown in Fig. 1.

Quasi-two-dimensional tumblers of radius $R=30$ mm and 45 mm having a glass front plate to allow optical access are filled with $d=0.53\pm0.05$ m glass beads and rotated at angular frequency ω (Fig. 2, inset). The tumblers have a thickness of $t=5$ mm$=9.4d$, wide enough to avoid jamming of the particles and narrow enough to be essentially two-dimensional. To minimize slippage of the granular bed with respect to the tumbler, the perimeter of the tumbler is covered with 60-grit sandpaper. The tumbler is supported at its circumference by a large ball bearing to withstand high g levels. The tumbler cell is mounted in a hinged capsule at the end of one of two opposing arms of the large centrifuge shown in Fig. 1. The radius from the centrifuge axis to the tumbler can be as large as 5.6 m, accounting for the position of the tumbler within the capsule and the angle of the capsule with respect to horizontal. The effective gravitational acceleration g_{eff} is directed perpendicular to the tumbler's axis and depends on the centrifuge's angular velocity, so g_{eff} can be varied between $1g$ and $25g$, where $g=9.81$ m/s^2.[1] This ratio of the highest to lowest effective gravities is a range comparable to that of the gravitational levels for the planets in the solar system.

The dynamic angle of repose β is a characteristic parameter of a flowing granular system that reflects the potential energy, frictional level, and particle characteristics of the surface flow. Figure 2 shows that the angle of repose of particles in a half-full 45-mm tumbler ($R/d=85$) increases with increasing tumbler rotational speed and decreases with increasing g level. This is consistent with previous results [10] for short-time experiments in a parabolic flight aircraft over a much narrower range of effective gravity from $0.02g$ to $1.8g$.

*Corresponding author. Electronic address: abrucks@uni-bremen.de
†Corresponding author. Electronic address: r-lueptow@northwestern.edu

[1]The motion of the particles in a centrifugal field gives rise to a Coriolis acceleration. This acceleration is less than $0.10g$ for low g levels and tumbler rotations rates, so its effect is assumed to be negligible in these cases (over 90% of the data). However, at the highest g levels and tumbler rotation rates, the Coriolis acceleration can be as much as $0.20g$.

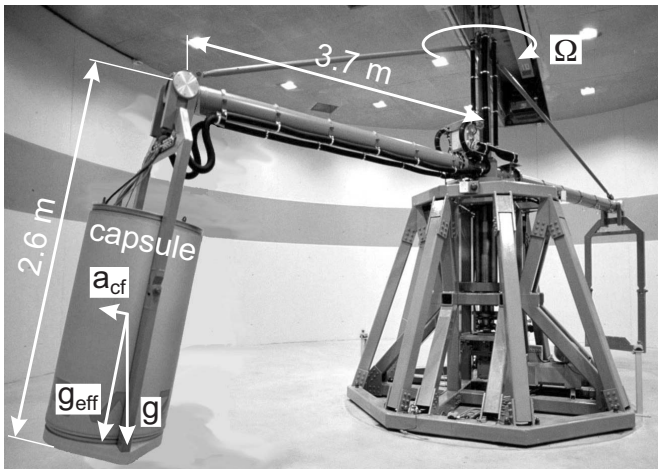

FIG. 1. The centrifuge facility at ZARM, University of Bremen.

However, the key result here lies in the scaling for the granular flow. The Froude number is the ratio of the centrifugal force due to rotation of the tumbler to the applied gravitational force due to the centrifuge rotation acting on the surface flow. When the angle of repose is plotted as a function of the Froude number, the data collapses for the full range of g levels for which the center portion of the flowing layer is flat and the angle of repose can be measured (solid curve in Fig. 3). Similar collapse occurs for the smaller-radius tumbler (dashed curve), though the curve is shifted to the right due to the smaller ratio $R/d=57$. The angle of repose asymptotes to the same value at low Froude numbers, probably because the particles are identical and the angle of repose for periodic avalanches is controlled by the particle size rather than the tumbler size.

The thickness of the flowing layer, δ, can be extracted by considering the portion of the particle bed showing straight particle streaks in time-lapse photos. Figure 4 provides examples of measurements of the flowing layer thickness for two very different Froude numbers. The flowing layer thickness in both cases is essentially independent of g_{eff},[2] consistent with a previous study focused on subsurface creeping flow [11]. These results suggest that the flowing layer dilates only enough to permit the motion of particles down the slope and is otherwise relatively unaffected by the gravitational level. The results also confirm the dependence of the shear rate on the gravitational level. For a half-filled tumbler, it can be shown that the shear rate is [11]

$$\dot{\gamma} \approx (R^2/\delta^2)\sqrt{(\mathrm{Fr}\, g_{eff}/R)}.$$

Since flowing layer thickness δ is independent of g_{eff} for a constant Froude number, the shear rate depends solely on the square root of the gravitational level, consistent with the theoretically predicted dependence of the shear rate or velocity on $\sqrt{g_{eff}}$ [12–14].

[2]The flowing layer thickness δ is also affected by the friction with and constraint by the tumbler side walls, but these effects do not alter the independence of δ with respect to g_{eff}.

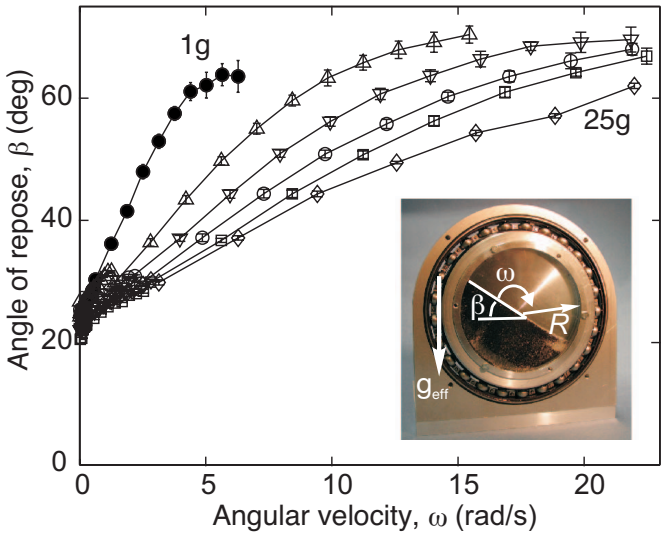

FIG. 2. (Color online) The dynamic angle of repose at the tumbler center increases with increasing angular velocity, yet decreases at high g levels. The tumbler radius is $R=45$ mm ($R/d=85$). Gravitational levels g_{eff}/g: (•) 1.00, (△) 5.04, (▽) 10.03, (○) 15.03, (□) 20.04, and (◇) 25.01. Standard deviation error bars are typically smaller than the symbols. Inset: angle of repose in the rotating tumbler half filled with $d=0.53$ mm beads. The surrounding ball bearing supports the tumbler at high g levels.

Several granular flow regimes can occur in a gravity-driven granular system [12,15–17]. Experiments at $1g$ over a wide range of rotational speeds and tumbler diameters have shown that material flows down the slope in discrete avalanches at the smallest Froude numbers. As the Froude num-

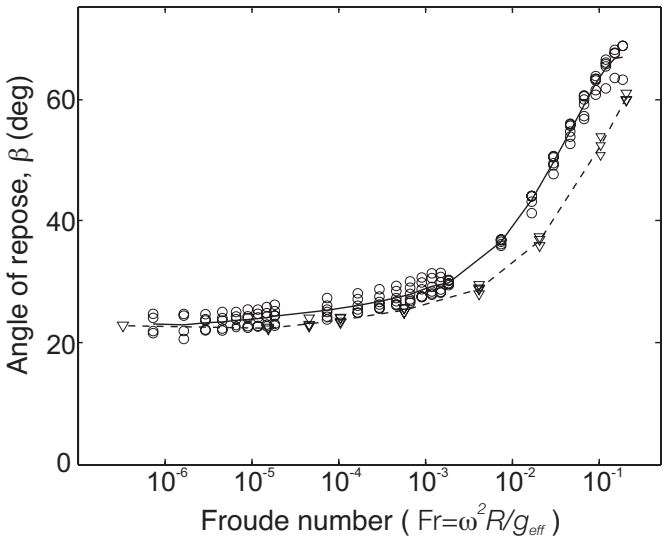

FIG. 3. Conditions at the different gravitational levels and angular velocities can be expressed in terms of the Froude number. The dynamic angle of repose data from Fig. 2 [(○) 45 mm radius tumbler, $R/d=85$] collapses into a single solid curve when plotted as a function of the Froude number. Data collapse onto a second curve when the geometric parameter is changed [(▽) 30 mm radius tumbler, $R/d=57$]. (○) At $g_{eff}/g=1.00$, 5.04, 10.03, 15.03, 20.04, and 25.01. (▽) At $g_{eff}/g=1.00$, 5.00, and 15.00.

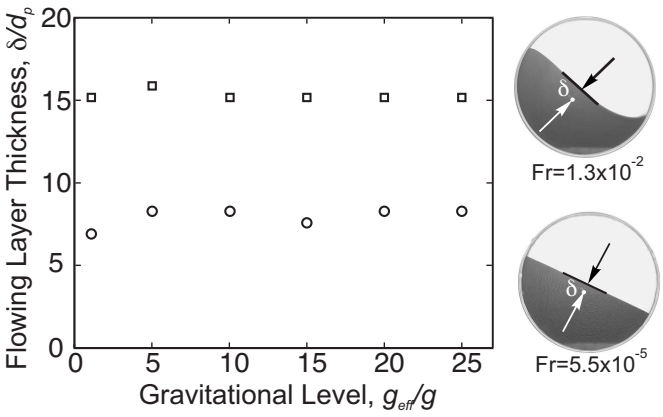

FIG. 4. The flowing layer thickness is essentially independent of the g level over a range of Froude numbers and flow states. [(○) $\mathrm{Fr}=5.5\times10^{-5}$, (□) $\mathrm{Fr}=1.3\times10^{-2}$].

ber increases, the flow becomes continuous, first with a flat surface (rolling flow) and then with a yin-yang-shaped surface (cascading flow). At high enough Froude numbers, the material is centrifuged to the periphery of the tumbler. Increasing the gravitational level for a constant rotational speed flattens the surface of the flowing layer as shown in the upper portion of Fig. 5. In this case ($\omega=0.3$ Hz $=1.885$ rad/s), the increase in g level from $1g$ to $25g$ takes the flow from the curved surface of cascading flow to the flat surface of rolling flow. However, for a constant Froude number, the shape of the flowing layer depends only on the Froude number, not directly on g_{eff}, as shown in the lower portion of Fig. 5. This is true over a range of Froude numbers

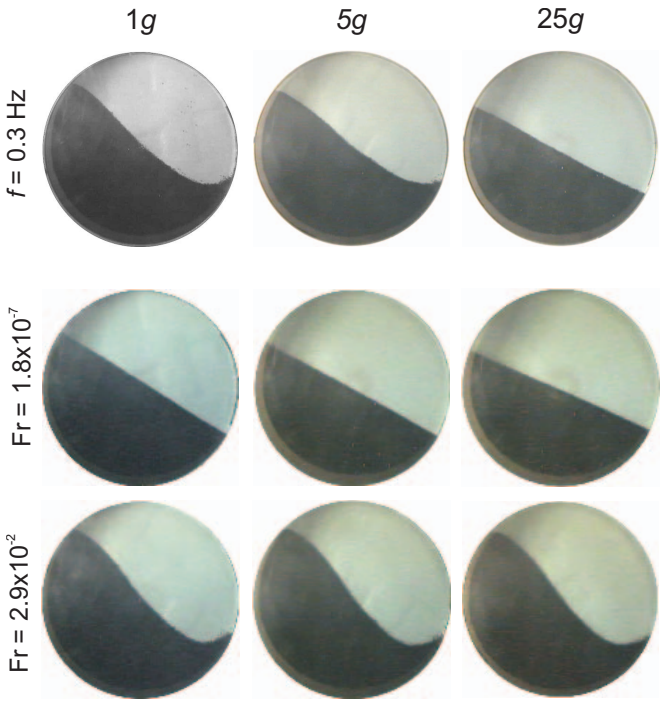

FIG. 5. (Color online) The surface of the flowing layer flattens as the g level increases (upper), but the shape of the flowing layer is consistent for a constant Froude number, regardless of the g level (lower).

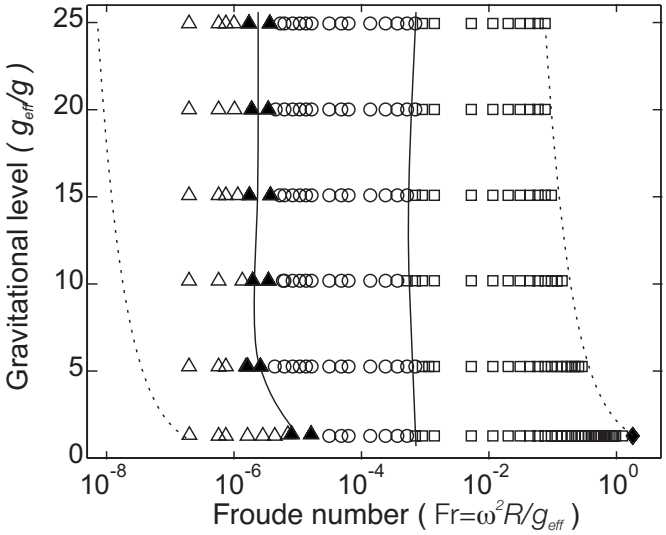

FIG. 6. With increasing Froude number, the flow passes through various flow states: avalanching (△), alternating between avalanching and rolling (▲), rolling (○), cascading (□), and centrifuging (◆). Except for the transition from avalanching to rolling at $g_{eff}/g\approx1$, the transitions are independent of the g level and depend only on the Froude number. The transitions are marked by solid curves to guide the eye. The dotted curves indicate the minimum and maximum Froude numbers that can be achieved with the setup.

from discontinuous avalanching flow to continuous cascading flow.

This result is further amplified by considering the state diagram of the flow regimes in the tumbler, shown in Fig. 6, which includes over 200 combinations of rotational speeds and gravitational levels. (Centrifuging of the granular material is only possible at the lowest g level due to constraints of the experimental apparatus.) The transition to the centrifugal regime of flow should depend only on the Froude number [18], but the dependence of other transitions, while assumed to be functions of the Froude number, have been shown to also depend to some extent on details of the experimental conditions, such as the radius of the tumbler or the size of the particles [12,15,17]. Figure 6 shows quite clearly that the boundaries between the flow regimes are generally vertical lines indicating that the nature of the flow depends primarily on the Froude number, regardless of the g level, with two caveats for the transition from avalanching to continuous flow. First, this transition is a bit fuzzy in that the flow alternates between the two states. In comparison, the flow does not alternate between states for the transition from rolling to cascading flow. Second, the transition at $1g$ occurs at a higher Froude number than for higher g levels. Experiments at $1.1g$ (with the centrifuge running) produce results nearly identical to those at $1.0g$, indicating that this is not a result of vibration of the centrifuge system disturbing the avalanche flow and causing transition to rolling flow earlier at higher g levels.

Tumbler results can be connected with chute and heap granular flows through the Froude number for these surface flows, $\mathrm{Fr}_{\mathrm{surf}}=u^2/\delta g_{eff}$, where u is a characteristic velocity of the flow [19,20]. Mass conservation in a tumbler requires that the average velocity in the flowing layer be $u=\omega R^2/2\delta$,

so that $\mathrm{Fr}_{\mathrm{surf}}=(R^3/4\delta^3)\mathrm{Fr}$. Our results indicate that Froude number properly accounts for the gravitational level in terms of the physical properties of the flow (angle of repose) and, to a large extent, the nature of the flow regimes that take place. Since the flowing layer thickness remains unaffected by the gravitational level, the velocity must scale with $\sqrt{g_{eff}}$ for constant Froude number. Of course, particle settling depends directly on g_{eff}. The combination of these effects points to longer lasting, but slower moving avalanches of similar size on the Moon or Mars as on Earth [4].

The key result here is that scaling relations for granular surface flows developed on Earth at $1g$ can be extended to other gravitational accelerations, when scaled according to the Froude number. Of course, several other issues come into play when considering lunar or Martian granular flows. First, granular flows can be influenced by the interstitial gas. On the Moon, avalanches would occur without interstitial gas. However, at pressures corresponding to atmospheric pressure on Mars, the influence of an interstitial gas on the flow may be significant [4,21]. Second, the particle size distribution and shape for lunar and Martian regolith range from fine dust to rocks and boulders [1,22,23], far from the ideal case of monodisperse, noncohesive, spherical particles used in these experiments. Furthermore, lunar regolith consists of jagged, sharp particles formed from constant bombardment by meteorites [22,23] that may interlock or break under flow. Clearly, the particle shape, frictional properties, and size distributions will affect the details of the flow. Nevertheless, the results presented here provide the starting point for further investigations of the effect of gravitational acceleration on the thickness, dilation, velocity, and shear in the flowing layer, as well as the nature of the creeping subsurface flow under varying levels of gravitational acceleration.

The authors thank the University of Bremen for funding this work.

[1] A. H. Treiman, J. Geophys. Res. **108**, 8031 (2003).
[2] M. F. Gerstell, O. Aharonson, and N. Schorghofer, Icarus **168**, 122 (2004).
[3] A. S. McEwan, Geology **17**, 1111 (1989).
[4] T. Shinbrot, N.-H. Duong, L. Kwan, and M. M. Alvarez, Proc. Natl. Acad. Sci. U.S.A. **101**, 8542 (2004).
[5] M. C. Malin, J. Geophys. Res. **97**, 16337 (1992).
[6] A. T. Basilevsky and J. W. Head, Rep. Prog. Phys. **66**, 1699 (2003).
[7] P. M. Schenk and M. H. Bulmer, Science **279**, 1514 (1998).
[8] K. A. Howard, Science **180**, 1052 (1973).
[9] J. D. Harrington, M. Braukus, and J. Dunn, URL http://www.nasa.gov/home/hqnews/2005/sep/HQ_05273_moon_dirt.html
[10] S. P. Klein and B. R. White, AIAA J. **28**, 1701 (1988).
[11] T. Arndt, A. Brucks, J. M. Ottino, and R. M. Lueptow, Phys. Rev. E **74**, 031307 (2006).
[12] J. Rajchenbach, Phys. Rev. Lett. **65**, 2221 (1990).
[13] S. Douady, B. Andreotti, and A. Daerr, Eur. Phys. J. B **11**, 131 (1999).
[14] D. V. Khakhar, A. V. Orpe, P. Andresen, and J. M. Ottino, J. Fluid Mech. **441**, 255 (2001).
[15] H. Henein, J. K. Brimacombe, and A. P. Watkinson, Metall. Trans. B **14B**, 191 (1983).
[16] J. M. Ottino and D. V. Khakhar, Annu. Rev. Fluid Mech. **32**, 55 (2000).
[17] J. Mellmann, Powder Technol. **118**, 251 (2001).
[18] G. H. Ristow, *Pattern Formation in Granular Materials* (Springer-Verlag, Berlin, 2000).
[19] O. Pouliquen, Phys. Fluids **11**, 1956 (1999).
[20] GDR MiDi, Eur. Phys. J. E **14**, 341 (2004).
[21] H. K. Pak, E. Van Doorn, and R. P. Behringer, Phys. Rev. Lett. **74**, 4643 (1995).
[22] D. S. McKay, G. Heiken, A. Basu, G. Blanford, S. Simon, R. Reedy, B. M. French, and J. Papike, in *Lunar Sourcebook*, edited by G. Heiken, D. Vaniman, and B. M. French (Cambridge University Press, New York, 1991), pp. 286–356.
[23] Y. Liu, J. Park, E. Hill, K. D. Kihm, and L. A. Taylor, in *Proceedings of the Tenth Biennial ASCE Aerospace Division International Conference on Engineering, Construction, and Operations in Challenging Environments*, Houston, TX, edited by R. B. Malla, W. K. Binienda, and A. K. Maji (American Society of Civil Engineers, Reston, VA, 2006).